Journal of Materials Chemistry B

Accepted Manuscript

ROYAL SOCIETY OF CHEMISTRY

www.rsc.org/materialsB

Journal Name

RSCPublishing

PAPER

One-pot green synthesis of water-soluble carbon nanodots with multicolor photoluminescence from polyethylene glycol

Cite this: DOI: 10.1039/x0xx00000x

Received filled in by the editorial staff,
Accepted filled in by the editorial staff

DOI: 10.1039/x0xx00000x

www.rsc.org/

Moyun Chen, Weizhi Wang*[a] and Xiaoping Wu*[b]

Water-soluble fluorescent carbon nanodots (CNDs) were fabricated directly from polyethylene glycol (PEG) by a simple one-pot thermal treatment. In such CNDs, PEG played two essential roles, carbon source and surface passivating agent. CNDs were used directly without any additional separation or purification procedure and yet have a comparable quantum yield with self-surface passivation CNDs or passivation-absent ones. The products were shown to be soluble in water and common organic solvents, and emitted bright multicolor fluorescence with excitation and pH dependent emission properties. The extensive characterization results likewise gave an insight into the formation and the luminescence mechanism of CNDs. The cytotoxicity test and cellular uptake experiments of CNDs further demonstrated their viability in biochemical applications.

1. Introduction

A great interest has been shown on fluorescent semiconductor nanoparticles such as CdTe and CdSe due to their unique optical and biochemical features.[1] However, these conventional semiconductors are generally made up of heavy metals which may be harmful towards mammalian cells and environment.[2] Therefore, the search for benign alternatives with excellent photoluminescence (PL) properties and low toxicity has been in progress. Carbon nanodots (CNDs) have attracted considerable attention owing to their notable PL properties, good bio-compatibility, chemical inertness and low cytotoxicity compared with metal-based quantum dots.[3] All these desirable properties encourage CNDs to develop a host of applications, for instance, bioimaging, biological labelling, drug delivery and fluorescent probe, in which size, biocompatibility and toxicity are of critical importance.[4-8]

Numerous routes to prepare CNDs have been reported, such as laser-ablation methods,[9] electrochemical synthesis,[10,11] microwave/ultrasonic synthesis[12-14] and combustion of carbon soot.[15] However, most of the above methods involve expensive starting materials, strong acid, sophisticated instruments and intricate process. The synthesized CNDs, typically, are always further surface passivated to improve the water solubility and PL properties which may limit their frequent applications. Therefore, serious efforts have been made to obtain self-passivated CNDs with a simple and green method. Liu *et al*.[6] fabricated polyethylenimine (PEI) functionalized carbon dots by one-step microwave assisted pyrolysis of glycerol and PEI mixture. Later on Mohapatra *et al*.[16] have produced highly green-fluorescent CNDs by one step hydrothermal treatment of orange juice at about 120 °C in 150 minutes. The most generally used starting material in these approaches is glucose and herein we present another abundant agent PEG as the only precursor.

PEG, a water-soluble polymer, has been the most popular surface passivating material and found to be effective in improving the solubility and biocompatibility of nano particles.[17] Moreover, PEG can be used for various biomedical applications due to its non-toxicity, non-immunogenicity and reactivity to other biomolecules.[18,19] In conclusion, PEG itself is a promising and attractive candidate in biological environment. However, PEG serves as both the source of carbon and the passivating agent is rarely proposed except that Jaiswal *et al*.[20] presented a methodology in which PEG acts as a dual role to form CNDs by microwave and later on Mitra *et al*.[21] described a synthetic approach for CNDs from PEG-200 after a sonication bath in the presence of NaOH. Nevertheless, these two methods either consumed a great deal of energy or needed extra additive and the products only emitted green or blue luminescence. On the other hand, neither of these two studies provided a deep insight into the structure and functional groups of the as-prepared products which are significant and fascinating.

Herein, we propose a convenient and simple one-step synthetic route for the preparation of luminescent CNDs from PEG at a comparatively low temperature (120-160 °C). Moreover, systematical investigation based on polyglycols including polypropylene glycol (PPG) and polytetramethylene

glycol (PTMG) have been carried out to explore the structural information and the formation mechanism of CNDs. In addition, CNDs reflected extended uses in cellular imaging, indicating the prospect of potential applications.

2. Experimental section

2.1. Chemicals

PEG-400, PPG-2000, sodium hydroxide (NaOH), ethanol, fluorescein, tetrahydrofuran (THF), toluene and sulfuric acid (H_2SO_4) were purchased from Sinopharm Chemical Reagent Co., Ltd (Shanghai, China). N-(3-dimethylaminopropyl)-N-ethylcarbodiime hydrochloride (EDC) and N-hydroxysuccinimide (NHS) were purchased from Aladdin Industrial Corporation (Shanghai, China). Goat antimouse secondary immunoglobulin G (IgG) was obtained from Boster Biotechnology (Wuhan, China). PTMG-1000, quinine sulfate, fluorescein isothiocyanate (FITC) and monoclonal anti-α-tubulin antibody were obtained from Sigma-Aldrich.

All chemicals and reagents used were of analytical grade and all chemicals were used as received without further purification. The solvents were used after purification according to conventional methods when required.

2.2. Synthesis of carbon nanodots (CNDs)

PEG-400 (10-15 mL) was added into a 50 mL reaction flask and heated by a preheated oil bath at 160 °C for a period of time (0.5h, 2h and 6h). It is found that experimental parameters such as reaction time have a distinct effect on the growth of CNDs; accordingly we can change parameters to prepare CNDs in a controllable way. After the heating process, the viscous liquid turned into low viscosity fluid and the color changed from transparent to pale yellow and finally became dark brown. Subsequently, the glass bottle was cooled to room temperature for further characterization. Besides PEG-400, we also investigate other polyglycols like PPG-2000 and PTMG-1000.

2.3. Measurements and characterization

^{1}H NMR spectra of the products were recorded on a JNM-MY60FT (JEOL, Japan) 500 MHz spectrometer. ^{13}C NMR spectra were measured on Varian Mercury Plus 400 spectrometer in deuterated chloroform or dichloromethane. Chemical shifts (δ) were referenced downfield from tetramethylsilane (TMS) using the residual solvent peak as an internal standard ($CDCl_3$, 7.23 ppm; CD_2Cl_2, 5.32 ppm). Polycyclic aromatic hydrocarbons (PAHs) were analyzed by Voyager DE-STR matrix assisted laser desorption time of flight mass spectrometry (MALDI-TOF). Raman experiment was performed using Labram-1B (Yobin Yvon, France) with excitation wavelength of 632.8 nm. Fourier transform infrared (FTIR) spectra of the samples were obtained using KBr disks by Nicolet 6700 spectrometer with a resolution of 4 cm^{-1}.

High-resolution transmission electron microscope (HRTEM) images were taken on a JEOL JEM2100 TEM instrument at an accelerating voltage of 200 keV. Dynamic light scattering (DLS) analysis was measured on a Zetasizer Nano ZS90 (Malvern Instruments, UK). The heights of CNDs samples were characterized by atomic force microscope (AFM) (Digital Instruments NanoScope IV and Bruker Multimode 8) operating in the tapping mode. Ultraviolet-visible (UV-vis) and PL spectra were recorded with a Perkin Elmer Lambda 35 spectrophotometer and an Edinburgh FLS920 spectrometer with Xe lamp as an excitation source, respectively. PL decay curves were recorded on FLS920 using a time-corrected single photon counting system.

2.4. Quantum yield measurements

Quantum yields were measured according to the established procedure[22] by using quinine sulfate in 0.1 M H_2SO_4 solution (η=1.33, Φ=55%) and fluorescein in 0.1 M NaOH solution (η=1.33, Φ=93%) as the reference respectively.[23] CNDs were dispersed in distilled water (η=1.33). Relative quantum yields of CNDs were calculated from the following formula:

$$\Phi_C = \Phi_S \frac{M_C \eta_C^2}{M_S \eta_S^2}$$

Where the subscript C and S denoted to CNDs samples and standard respectively, Φ was the quantum yield, M was the slope from the plot of the integrated fluorescence intensity versus absorbance, and η was the refractive index of the solvent.

2.5. Cell viability assay

HeLa cells were cultured in a RPMI-1640 medium supplemented with 10% fetal calf serum (FCS, Gibco BRL), penicillin 100 U mL^{-1}, streptomycin 100 μg mL^{-1} and 1% glutamine (Gibco BRL) in 5% CO_2 at 37 °C. Prior to being tested, cells were seeded in 96-well plates (Gibco BRL) at an initial density of 1×10^5 cells per mL for 24 hours. Dilution of CNDs was then added to RPMI-1640 medium and incubated for another 24 hours. Afterwards, the medium was aspirated and 100 μL fresh medium containing 10% FCS was added to each well with 10 μL 3-(4,5-dimethylthiazol-2-yl)-2,5-diphenyl-2*h*-tetrazoliumbromide (MTT, Sigma) stock suspension (5mg mL^{-1}) and incubated for 4 hours at 37 °C. Subsequently, the medium was removed and the formazan crystals were dissolved in 100 μL dimethylsulfoxide (DMSO) per well. A Molecular Devices SpectraMax M5 Microplate Reader was used to measure the absorbance at 490 nm. The viability of the HeLa cells exposed to the CNDs was expressed as a relative percentage as normalized to the untreated control which was set as 100%. All the records were explained as average data with error bars.

2.6. Immunofluorescnet measurement

2.6.1. Preparation of CNDs/Antibody Conjugates

The CNDs are readily conjugated to goat antimouse IgG through amidation by using EDC/NHS as zero length cross-linkers. 16 μL EDC (6.4 mg mL^{-1} in phosphate buffer solution

(PBS), 0.01M, pH=7.4) was added to 100 μL CNDs. Then the solution was kept at 25 °C for 15 min to completely activate the carboxylic acid groups. Then 4μL NHS and 80 μL goat antimouse IgG (4 mg mL^{-1} in PBS, 0.01M, pH=7.4) were added successively under shaking. The mixed solution was placed at 25 °C for 2 h under dark. Subsequently, the resultant solution was incubated at 4 °C for 24 h. Afterwards, the solution was purified by using 300 kDa Nanosep centrifugal devices through centrifugation at 5000 rmp for 20 min. The products were stored at 4 °C in the dark.

2.6.2. In situ immunofluorescent measurements

Cell lines A549 (lung cancer cells) were obtained from American Type Culture Collection and cultured under conditions provided by the manufacturer. Firstly, cell lines A549 were cultured in complete RPMI 1640 (Invitrogen) supplemented with 10% fetal calf serum, 1% penicillin and streptomycin. Afterwards, they were maintained at 5% CO_2 humid atmosphere at 37 °C.

Cells were grown on glass coverslips for 36 h and were fixed in 4% paraformaldehyde for 10 min, then permeabilized with 0.1% Triton X-100 for 15 min at room temperature. The coverslips were blocked in 10% goat serum for 1 h at room temperature and subsequently incubated with a monoclonal antibody against human α-tubulin (1:200) for overnight at 4 °C. After extensive washing in PBS, samples were further incubated with CNDs conjugated goat anti-mouse IgG (1:50) and 4',6-diamidino-2-phenylindole (DAPI) (0.1 μg mL^{-1}) for 1 h. After extensive washing, the samples were examined by the confocal microscope (LSM 710, Zeiss, Germany).

3. Results and discussion

3.1. Synthesis

CNDs were prepared by a simple thermal decomposition route without further modification steps. The only reagent was polyglycol (PEG, PPG or PTMG), acting as both the carbon resource and the passivation agent, which made this method fascinating when compared with other CNDs preparations. Faint yellow liquid containing CNDs was obtained after a period time of heating. Significantly, as-prepared products emitted green to orange fluorescence when irradiated with a UV lamp (Fig. 1) and they didn't have any perceptible change three months later at room temperature, thus imparting them with good stability. Interestingly, when the whole procedure was under the protection of N_2, the formation of CNDs consumed much more time. What's more, an attractive phenomenon was observed when we treated PEG, PPG and PTMG with the same heating time and temperature. Fig. S1 of Supporting Information (SI) shows products originated from PEG, PPG and PTMG respectively. It reveals that the starting material with higher oxygen to carbon ratio (O/C) is easier to form CNDs. Thus it helps us penetrate into the formation of CNDs.

Here we could draw a conclusion that three key factors, heating time, existence of oxygen and O/C ratio, act critical

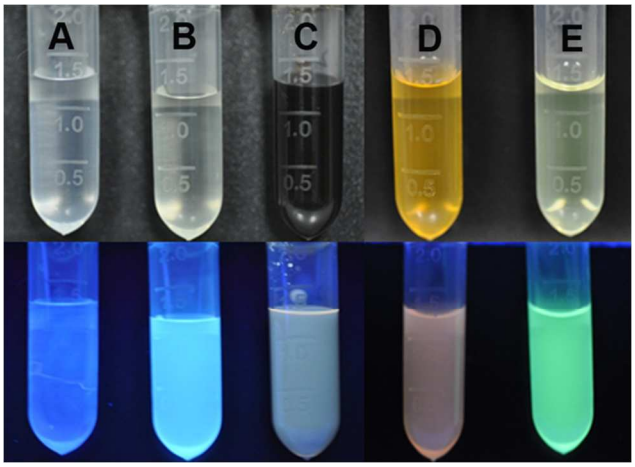

Fig. 1 Photograph of CNDs under sunlight (top) and 365 nm UV light (bottom). (A) raw PEG, (B) CNDs originated from PEG by heating for 0.5 h, denoted as e-CNDs@0.5h, (C) CNDs originated from PEG by heating for 6 h, denoted as e-CNDs@6h, (D) CNDs originated from PEG and PAHs mixture by heating for 2 h, denoted as e-PAHs-CNDs@2h, dispersed in water and (E) e-PAHs-CNDs@2h, dispersed in ethanol.

roles in the fabrication of CNDs. For reference, we proposed a tentative mechanism of CNDs formation depicting in Scheme 1. It shows that PEG molecules were firstly pyrolyzed and oxidized, then grew into clusters and finally converted to CNDs. We will discuss the formation mechanism with robust evidence in the following section.

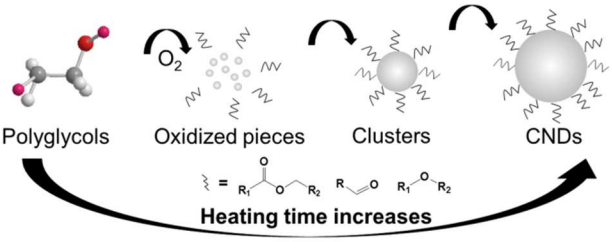

Scheme 1 Formation of CNDs.

Conventional quantum dots have a typical quantum confinement and exhibit strictly size-dependent fluorescence so that it is cushy to tune the color of QDs simply by controlling particle size,[24] whereas carbon nanodots do not firmly obey the rule. Consequently, carbon nanoparticles are not considered as carbon quantum dots but carbon nanodots. The fluorescent mechanism is still an open question, for which there are several suggestions come up by the researchers, such as emissive traps and the radiative recombination of excitions.[25,26] The color of the photoluminescence is not only determined by different sizes but also different surface trap sites. Besides, CNDs produced by different methods have diverse elucidations of fluorescence

mechanism. Throughout previous studies, CNDs emitting green and blue fluorescence are easy to obtain, whereas yellow and other colors with longer wavelength are rarely achieved.[27-30]

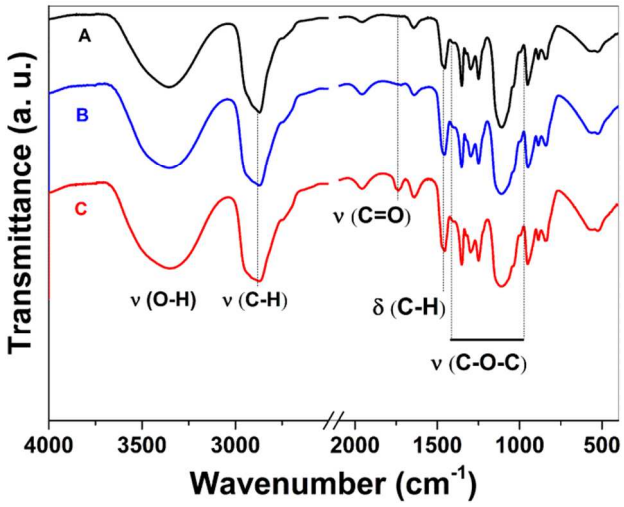

Fig. 2 FTIR spectra of (A) raw PEG, (B) e-CNDs@0.5h and (C) e-CNDs@6h.

To solve this problem, we mixed PAHs, consisting of structurally similar multiple benzene rings (Scheme S1), with PEG to prepare red fluorescence CNDs. PAHs are the particular chemicals we have synthesized and characterized (Scheme S1) and can offer cores for the growth of CNDs. On the other hand, PAHs are nonpolar and hydrophobicity which highly limits the use especially in the biological field. Nevertheless, PEG is hydrophilic and we can expect the products may have an improved water-solubility thus affords its possible use in aqueous systems. Fig. 1 shows PEG-PAHs based CNDs in water and ethanol under a UV lamp. It reveals that the products have excellent solubility in water and ethanol, while pure PAHs are insoluble in aqueous solution. Besides, it emitted red color in water and green color in ethanol which largely enriched the fluorescent color of CNDs. The reason lies in the aggregation of PAHs in different polar solvents.

3.2. Characterization

FTIR spectroscopy was used to investigate the functional groups of the CNDs as shown in Fig. 2 and Fig. S4. The peak at 1738 cm^{-1} attributed to C=O stretching becomes stronger as the heating time increased. It hints that during thermal oxidation, oxygen containing groups like carboxyl and carbonyl were introduced to CNDs. One broad peak around the range of 3000-2670 cm^{-1} and a sharp peak at 1457 cm^{-1} are ascribed to the vibration and deformation bands of C-H. The broad peak centered at 3362 cm^{-1} originates from the stretching vibration of O-H. The stretching vibration of C-O-C can be characterized by multi peaks in the region of 1400-1000 cm^{-1}.

To further confirm the chemical structure of CNDs, ^{1}H NMR spectra were carried out as presented in Fig. 3a and Fig. S5. The ^{1}H NMR spectra reveal remarkable changes in three regions which are: 9-7 ppm (for the aromatic or sp^2 protons), 5.5-4.0 ppm (for the protons attached with hydroxyl, ether or carbonyl groups) and 2.5-1.0 ppm (for the protons adjoin the

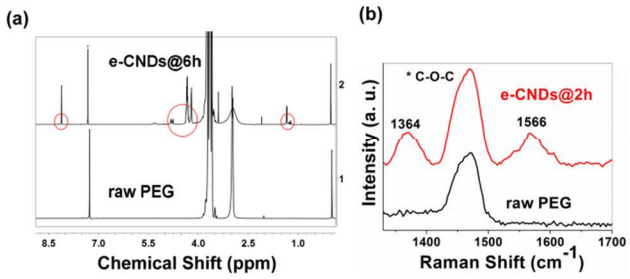

Fig. 3 (a) ^{1}H NMR spectra and (b) Raman spectra of raw PEG and CNDs prepared with different heating times

aromatic or sp^2 protons), respectively.[31] The functional groups of the CNDs determined by ^{1}H NMR are in good agreement with FTIR results.

Moreover, Raman spectroscopy is a powerful tool to characterize the carbon-based materials; Fig. 3b displays the Raman spectra of raw PEG and CNDs. The crystalline *G* band at 1566 cm^{-1} and the disordered *D* band at 1364 cm^{-1} can be found in Fig. 3b easily, which are in conformity with the main features in the Raman spectra of carbons.[32] The relative integrated area of *D* band to *G* band (I_D/I_G) of CNDs sample is 0.84, which is higher than CNDs fabricated by electrochemical synthesis.[33] The high ratio (I_D/I_G) reveals a significant number of oxygen containing functional groups, which have been substantiated by FTIR and ^{1}H NMR, attached to the surface of as-prepared CNDs and also confirm that the core/shell structure has a relative thick shell compared to the small core, in accordance with the structure and formation mechanism we proposed in Scheme 1. Furthermore, the presence of these carbonyl moieties not only provides a deep insight into the fluorescence mechanisms of CNDs, but also imparts the

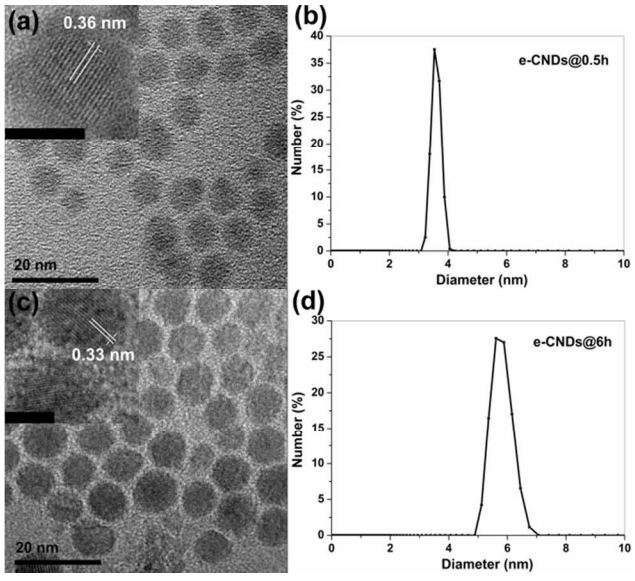

Fig. 4 (a) HRTEM images of e-CNDs@0.5h (inset scale bar: 5 nm), (b) DLS result of e-CNDs@0.5h, (c) HRTEM images of e-CNDs@6h (inset scale bar: 5 nm, (d) DLS result of e-CNDs@6h.

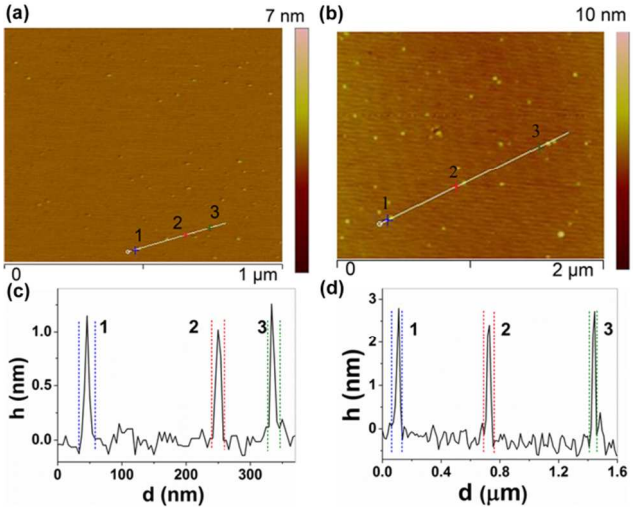

Fig. 5 AFM topography images of (a) e-CNDs@0.5h, (b) e-CNDs@6h and height distributions of (c) e-CNDs@0.5h and (d) e-CNDs@6h.

products with outstanding water-solubility and suitability for subsequent functionalization which are extremely important for biological applications.

Fig. 4, Fig. S6 and Fig. S7 show the TEM images, HRTEM images, size distribution and DLS results of CNDs. It can be clearly observed that the as-prepared CNDs are spherical and well dispersed. Moreover, the inset in Fig. 4a and 4c reveal the high crystallinity of CNDs and demonstrate the lattice spacing of 0.33 nm and 0.35 nm which correspond to the 002 lattice planes of graphitic carbon.[34,35]

According to the size distribution depicted in Fig. S6, the average diameter of e-CNDs@0.5h and e-CNDs@6h are approximately 2.3 nm and 4.7 nm, respectively. The corresponding DLS results in Fig. 4b and 4d confirm that the hydrodynamic diameters of e-CNDs@0.5h and e-CNDs@6h are about 3.6 nm and 5.8 nm, respectively. The different diameters measured by DLS and TEM are attributed to the different surface states of CNDs under the two measurement conditions. Under the TEM measurement condition, the solvent in the samples is removed, as for DLS, samples are dispersed in good solvent, thus yielding a larger diameter than which characterized by TEM.[36,37] Besides, the results also verify that the heating time does play a key role in the growing of CNDs as we predicted before.

AFM images in Fig. 5 demonstrate topographic morphology of as-prepared CNDs. As exhibited in Fig. 5c, the heights of e-CNDs@0.5h are approximately 1.5 nm, while the heights reach around 2.5 nm as heating time prolonged to 6 h according to Fig. 5d. Significantly, AFM images show that precipitates are monodisperse which could be contributed to the simultaneous and homogeneous heating of the sole material, and thus offers uniform nucleation for CNDs to grow concurrently.

TEM and AFM results indicate a positive correlation between the size of CNDs and heating time. Combined with structural information and the results of the contrast experiments, we proposed an oxidation mechanism as displayed in Scheme 1. At first, chain cleavages and oxidation take place in the presence of oxygen, resulting in carbon-carbon double bonds and carbonyl groups as revealed by FTIR and ^{1}H NMR. The possible process of chain cleavage and oxidation is proposed in Scheme 2. Carbon radicals are generated by heating and oxygen is added to the radical, forming unstable peroxides which will lose hydroxyl radical quickly. Subsequently, C-O bond cleavages take place, resulting in carbonyl groups and polymeric radicals.[38] Polymer radicals then abstract hydrogen and form C=C through dehydration. The chains containing carbon-carbon double bonds are apt to gather and fabricate hydrophobic cores and they grow larger as more C=C even aromatic rings are generated by dehydration and oxidation process, while O-related groups also reach to the surface of the cluster and form surface passivation layers. Eventually, core-shell structured CNDs as we described in Scheme 1 are obtained with the heating time increasing.

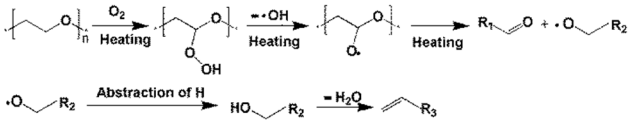

Scheme 2 Chain cleavage and oxidation.

3.3. Optical properties

Photophysical properties of as-formed CNDs were investigated afterwards. According to the UV-vis spectrum of CNDs dispersed in deionized water (Fig. 6 and Fig. S8a), the peak centered at 246 nm is due to π-π* transition of C=C, while the bulge at 310 nm is attributed to n-π* transitions of C=O and it is almost covered by the broad peak of π-π* transition in UV-vis spectrum of e-CNDs@6h sample.[39] It should be noted that compared with the reported studies the peaks of featured bonds red-shifted, which may attribute to the structure with larger conjugation.[14] Since as-prepared CNDs have a quite extraordinary stability, UV-vis properties were almost unaltered at any pH, ranging from 1 to 11 (Fig. S8b).

To gain greater insight into the fluorescence of CNDs, 2D-fluorescence topographical maps of CNDs were carried out as

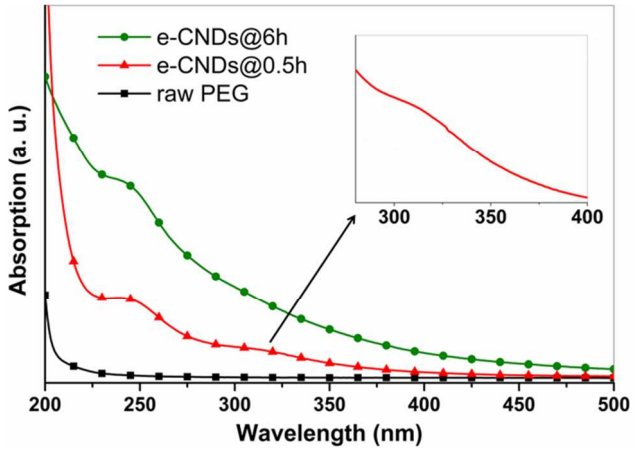

Fig. 6 UV-vis absorption spectra as a function of heating time.

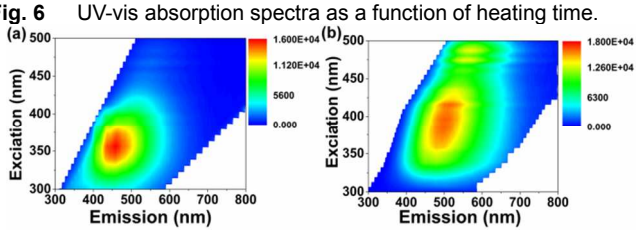

Fig. 7 2D-fluorescence topographical map of (a) e-CNDs@0.5 h and (b) e-CNDs@6 h, dispersed in distilled water.

shown in Fig. 7 and Fig. S10. The images show that the emission peak shifts from 450 nm to 500 nm as the heating time increase, indicating CNDs with longer heating time contain larger conjugated structures, which is accordance with the formation mechanism we put up in Scheme 1. Furthermore, in both samples, e-CNDs@0.5h and e-CNDs@6h, the maximum emission intensity red shift as excitation wavelength increases. Significantly, a comparison between e-CNDs@0.5h and e-CNDs@6h shows that the maximum emission region (painted red in Fig. 7) in e-CNDs@0.5h is centralized while in e-CNDs@6h is broad and has a higher red shift and even shifts to the red region (600 nm). According to the preparation procedure, these two samples are originated from the same starting materials and under the same procedure, the only difference between these two samples is the increasing heating time which is expected to generate large sized CNDs with extended distribution. Hence, the reason of the different 2D-fluorescence features is speculated on the broader size distribution of e-CNDs@6h. In addition, the excitation wavelength (λ_{ex}) dependent PL behavior is a typical property of CNDs, and there are several explanations proposed like the optical selection of different sized CNDs, different emissive traps and other mechanisms.[40,25,41,3] According to the preparation procedure and former characterization results of these two samples, we believe that the phenomenon also arises due to the different sized CNDs. Moreover, we investigated the pH effect of the fluorescence as shown in Fig. S11. It is noteworthy that CNDs are stable at the physiological and pathological pH range of 5-10 with a slightly alteration in fluorescence intensity, but decrease pronouncedly in acidic and strong basic regions. The decrease may be attributed to the change of the environment around the passivated surface.[26]

Moreover, the as-prepared CNDs exhibit remarkable photostability as compared to regular fluorescent chemicals like FITC. As shown in Fig. 8, the fluorescence of FITC is quenched in less than 5 min under UV irradiation, while the fluorescence of CNDs is extraordinarily stable for at least 60 min under the same irradiated condition. The striking photostability of CNDs is due to the protective shell, similar to silicon quantum dots.[42] Remarkably, the as-prepared CNDs maintain the fluorescent properties after storage in the ambient environment for 1 month (Fig. S12). All above features guarantee CNDs attractive candidates for biomedical uses.

As shown in Fig. S13 and Table S1, quantum yields (QYs) of the products are higher than those of self-passivated CNDs or

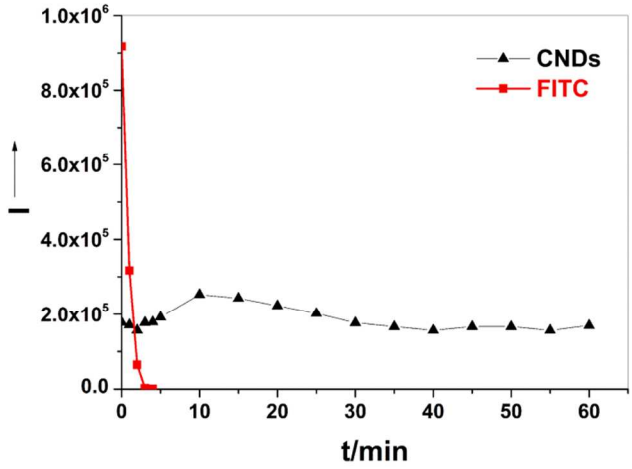

Fig. 8 Photostability comparison of FITC and as-prepared CNDs. All samples are continuously irradiated by a 1 kW high-pressure mercury lamp.

passivation-absent ones.[15,21] It reflects the connatural constructions of CNDs, ascribed to the inner structure relied on

Table 1 Parameters and average lifetimes of CNDs.[a]

	τ_1/ns (%)	τ_2/ns (%)	$\tau_{average}$ /ns
e-CNDs@0.5h in toluene	1.60 (66.92)	5.82 (33.08)	3.00
e-CNDs@0.5h in ethanol	1.78 (66.66)	6.18 (33.34)	3.25
e-CNDs@0.5h in H_2O	1.73 (53.93)	6.96 (46.07)	4.14
e-CNDs@6h in H_2O	2.57 (47.66)	9.07 (52.34)	5.97

[a] The fluorescence decay curves fit into a two-exponential function: $I(t) = A + B_1 e^{-t/\tau_1} + B_2 e^{-t/\tau_2}$, and the average lifetime is calculated according to $\tau_{average} = \sum B_i \tau_i$.

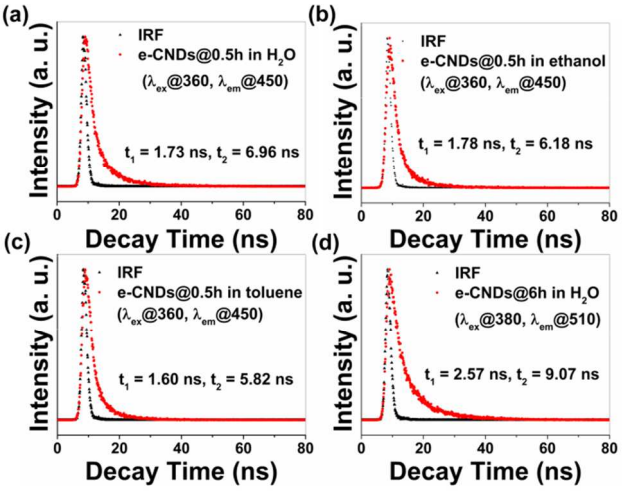

Fig. 9 PL decay profile of CNDs. e-CNDs@0.5h in (a) water, (b) ethanol and (c) toluene respectively, monitoring the emission at 450 nm with 360 nm excitation and (d) e-CNDs@6h in water, monitoring the emission at 510 nm with 380 nm excitation.

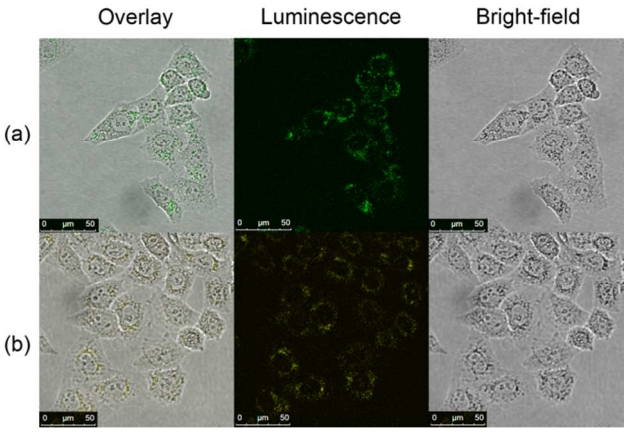

Fig. 10 Confocal luminescence images of HeLa cell treated with CNDs. (a) e-CNDs@0.5h and (b) e-CNDs@6h.

the fabrication techniques or starting materials.[43]

Fig. 9 represents time-resolved decay profiles of CNDs which show double exponential decay kinetics. Parameters calculated from the reconvolution of the decay with the instrument response function (IRF) contain a fast component and a slow component as summarized in Table 1. Mechanically, the double de-excitation processes of the CNDs are attributed to a fast band gap transition and long decay of oxygen-related emission.[43] Besides, the average lifetimes of e-CNDs@0.5h in different solvents are changing from 3 ns to 4.14 ns (Table 1) as the polarity of the solvent increases. The different dynamic behaviors of CNDs in these solvents are related to the surface functional groups, as characterized before, carbonyl and hydroxyl, which make CNDs have good solubility in polar solvent like water and nonpolar the opposite. We deduce this phenomenon is associated with aggregation state of CNDs in different polar solvents, and as we know aggregation causes quenching according to the reports.[44] More importantly, lifetime of CNDs in nanosecond indicates that the products are most appropriate for optoelectronic and biological applications.[45] What's more, the fluorescence lifetimes of CNDs we obtained by one-step thermal synthesis are longer than those prepared by microwave-assisted pyrolysis method.[46]

3.4. Potential applications in biology

Fluorescent nanoparticles have attracted increasing research attention due to their promising applications in bionanotechnology. To date, there have developed a variety of nanoparticle-based fluorescent probes, for instance, semiconductor quantum dots, nanodiamonds and silicon-based nanoparticles (SiNPs). However, these materials have restrictions of one kind or another. Semiconductor quantum dots raise concerns over toxicity and environmental harm.[2] As for nanodiamonds, they are generally obtained from milling microdiamonds, chemical vapor deposition, shockwave or detonation process.[3] Consequently, nanodiamonds typically exist as strongly bound agglomerates due to the harsh conditions in the reaction chamber. What's worse, the

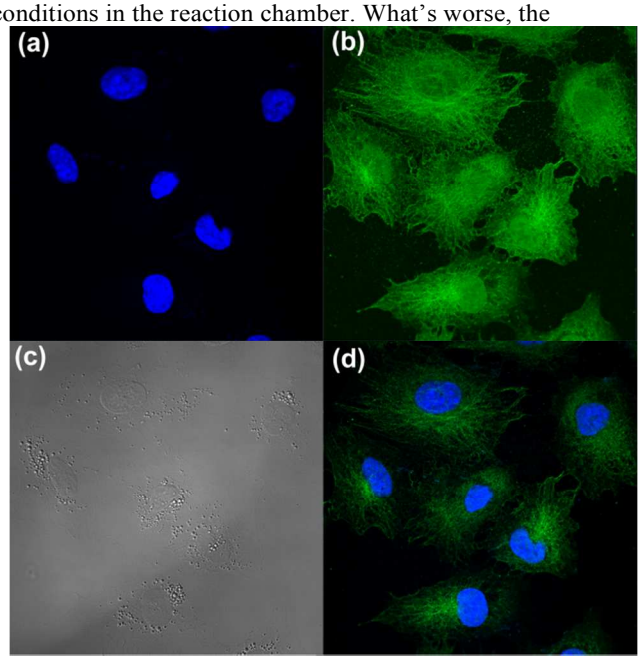

Fig. 11 Immunofluorescent cell images. (a) nuclei are distinctively labled by DAPI (excitation: 405 nm, detection window: 420-490 nm); (b) microtubules are distinctively labeled by CNDs (excitation:488 nm detection window: 510-560 nm); (c) bright-field of the cells; (d) overlaid image of (a) and (b).

diamonds are not only connected by noncovalent interactions, but also covalent bonds.[47] Therefore, preparation of nano-scaled deagglomeration nanodimonds appropriate for biolabels is a challenging task. In addition, the centres in the nanodiamonds responsible for fluorescence are the products of irradiation followed by thermal annealing at high temperatures (e.g. 800 °C).[48] The rigorous condition and energy-consuming process partly limit their applications. SiNPs also offer

potential for biomedical applications. However, most as-prepared SiNPs have poor water-dispersibility due to their hydrophobic surfaces covered by Si-H and require additional surface modification.[49] Apart from that, SiNPs often show obvious PL degradation, especially in biological media with different pH, which severely hinder their broad applications in biology.[50] In recent years, researchers have made persistent efforts to solve these problems. For instance, He's group has developed several unique microwave-assisted strategies to prepare water-dispersible, pH-stable and strong-fluorescent SiNPs, which made a great step in the biological application.[51,52] Considering the facile preparation process, suitable nano-scaled size, remarkable fluorescent properties, excellent water-solubility, photo-/storage stability in biological media and low-toxicity starting material, CNDs are attractive alternatives for cellular imaging.

In vitro bioimaging and cell viability were assessed with HeLa line. As shown in Fig. 10, confocal fluorescent images of HeLa cells incubated with two kinds of CNDs for 24 h, bright green and yellow luminescence are observed inside the cells,

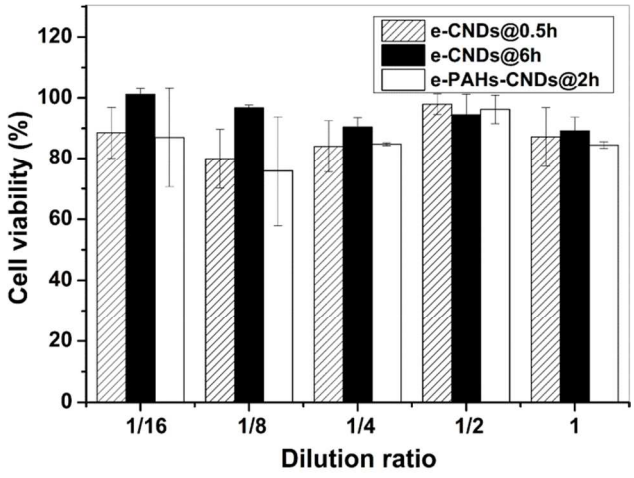

Fig. 12 Cytotoxicity test of CNDs based on dilution ratios with HeLa cells. The original concentrations of the CNDs are 50 mg mL^{-1} (left, e-CNDs@0.5h), 2.5 mg mL^{-1} (middle, e-CNDs@6h) and 25 mg mL^{-1} (right, e-PAHs-CNDs@2h), respectively.

respectively, and mainly localized in the cytoplasm regions so that the morphology of the cells can be distinguished clearly with the internalized CNDs. This result connotes that CNDs easily entered into HeLa cells through endocytosis but did not penetrate into the nuclei,[53] indicating CNDs didn't cause genetic disruptions of the living cells.[4]

Besides, CNDs readily react with amino groups of the secondary antibody via EDC/NHS cross-linking reaction. The resultant fluorescent bioconjugates are further supplied for immunofluorescnet cell labelling. On the basis of the specific antibody-antigen immunoreactions, the conjugates are specifically targeted to the microtubules of lung cancer cells A549, which are incubated with a monoclonal antibody against human α-tubulin. Fig. 11 shows A549 cells were dually stained by CNDs conjugates and DAPI, a cell-nucleus dye, with a high spatial resolution. The nuclei and microtubules were clearly labeled by the blue-colored DAPI (Fig. 11a) and the green-colored CNDs conjugates (Fig. 11b), respectively. Significantly, the PL of the double stained cells is distinctive and clearly spectrally resolved.

In biomedical applications especially in live cell related uses, the cytotoxicity is an imperative factor. The toxicity of as-prepared CNDs was carried out by MTT based cell viability assay as described in the Experimental section. MTT assay is a simple, precise and commonly used technique to detect living cells in mammalian cell cultures.[54] It is remarkable to notice that even the concentration of CNDs was 50 mg mL^{-1} with e-CNDs@0.5h and 2.5 mg mL^{-1} with e-CNDs@6h, the survival rates of the cells achieve as high as 80% (Fig. 12).

4. Conclusions

In summary, we have developed a facile, green and one-step method to prepare multi-color luminescent CNDs using a sole precursor PEG without any additive reagent and further treatment. PEG is widely used as surface passivation agent and it has remarkable properties in biology fields such as cost-effective, water-solubility and reactivity to many biomolecules. The formation mechanism of CNDs was proposed and testified by robust proof. Size and fluorescence color selective CNDs can be roughly obtained by adjusting the heating time. As-prepared CNDs exhibit excellent water-solubility, photo-/environmental stability, excitation and pH dependent luminescence, low cytotoxicity and a nanosecond-grade lifetime. The cellular uptake experiment illustrates that CNDs can serve as an ideal indicator for biomedical applications. As PEG is active to other biomolecules, further conjugation of CNDs with antibodies, drug molecules and other biomolecules can be viable, opening a window to a variety uses such as drug delivery, targeting therapy and bioimaging.

Acknowledgements

This work was financially supported by the National Nature Science Foundation of China (20704009, 21274027and 31101573).

Notes and references

[a] *State Key Laboratory of Molecular Engineering of Polymers, Department of Macromolecular Science, Fudan University, Shanghai, China, 200433. E-mail: weizhiwang@fudan.edu.cn*

[b] *State Key Laboratory of Genetic Engineering, School of Life Sciences, Fudan University, Shanghai, China, 200433, wuxp@fudan.edu.cn*

† Electronic supplementary information (ESI) available. See DOI: 10.1039/b000000x/

1 P. Alivisatos, *Nat. Biotechnol.*, 2004, **22**, 47-52.
2 J. Gao and B. Xu, *Nano Today*, 2009, **4**, 37-51.
3 S. N. Baker and G. A. Baker, *Angew. Chem. Int. Ed.*, 2010, **49**, 6726-6744.

4 M. Zhang, L. Bai, W. Shang, W. Xie, H. Ma, Y. Fu, D. Fang, H. Sun, L. Fan, M. Han, C. Liu and S. Yang, *J. Mater. Chem.*, 2012, **22**, 7461-7467.
5 S. Qu, X. Wang, Q. Lu, X. Liu and L. Wang, *Angew. Chem. Int. Ed.*, 2012, **51**, 12215-12218.
6 C. Liu, P. Zhang, X. Zhai, F. Tian, W. Li, J. Yang, Y. Liu, H. Wang, W. Wang and W. Liu, *Biomaterials*, 2012, **33**, 3604-3613.
7 C. W. Lai, Y. H. Hsiao, Y. K. Peng and P. T. Chou, *J. Mater. Chem*., 2012, **22**, 14403-14409.
8 Q. Li, T. Y. Ohulchanskyy, R. Liu, K. Koynov, D. Wu, A. Best, R. Kumar, A. Bonoiu P. N. Prasad, *J. Phys. Chem. C*, 2010, **114**, 12062-12068.
9 S. T. Yang, L. Cao, P. Luo, F. Lu, X. Wang, H. Wang, M. J. Meziani, Y. Liu, G. Qi and Y. P. Sun, *J. Am. Chem. Soc.*, 2009, **131**, 11308-11309.
10 J. Zhou, C. Booker, R. Li, X. Zhou, T. K. Sham, X. Sun and Z. Ding, *J. Am. Chem. Soc*., 2007, **129**, 744-745.
11 H. Ming, Z. Ma, Y. Liu, K. Pan, H. Yu, F. Wang and Z. Kang, *Dalton Trans.*, 2012, **41**, 9526-9531.
12 H. Zhu, X. Wang, Y. Li, Z. Wang, F. Yang and X. Yang, *Chem. Commun*., 2009, 5118-5120.
13 H. Li, X. He, Y. Liu, H. Huang, S. Lian, S. T. Lee and Z. Kang, *Carbon*, 2011, **49**, 605-609.
14 L. Tang, R. Ji, X. Cao, J. Lin, H. Jiang, X. Li, K. S. Teng, C. M. Luk, S. Zeng, J. Hao and S. P. Lau, *ACS Nano*, 2012, **6**, 5102-5110.
15 H. Liu, T. Ye and C. Mao, *Angew. Chem. Int. Ed.*, 2007, **46**, 6473-6475.
16 S. Sahu, B. Behera, T. K. Maiti and S. Mohapatra, *Chem. Commun.*, 2012, **48**, 8835–8837.
17 R. Liu, D. Wu, S. Liu, K. Koynov, W. Knoll and Q. Li, *Angew. Chem.*, 2009, **121**, 4668-4671.
18 F. M. Veronese and G. Pasut, *Drug. Discov. Today*, 2005, **10**, 1451-1458.
19 A. S. Karakoti, S. Das, S. Thevuthasan and S. Seal, *Angew. Chem. Int. Ed.*, 2011, **50**, 1980-1994.
20 A. Jaiswal, S. S. Ghosh and A. Chattopadhyay, *Chem. Commun.*, 2012, **48**, 407-409.
21 S. Mitra, S. Chandra, S. H. Pathan, N. Sikdar, P. Pramanik and A. Goswami, *RSC Adv.*, 2013, **3**, 3189-3193.
22 M. Grabolle, M. Spieles, V. Lesnyak, N. Gaponik, A. Eychmüller and U. Resch-Genger, *Anal. Chem.*, 2009, **81**, 6285-6294
23 J. N. Demas and G. A. Crosby, *J. Phys. Chem*., 1971, **75**, 991-1024.
24 A. P. Alivisatos, *Science*, 1999, **271**, 931-937.
25 Y. P. Sun, B. Zhou, Y. Lin, W. Wang, K. A. S. Fernando, P. Pathak, M. J. Meziani, B. A. Harruff, X. Wang, H. Wang, P. G. Luo, H. Yang, M. E. Kose, B. Chen, L. M. Veca and S. Y. Xie, *J. Am. Chem. Soc.*, 2006, **128**, 7756-7757.
26 R. Liu, D. Wu, S. Liu, K. Koynov, W. Knoll and Q. Li, *Angew. Chem. Int. Ed.*, 2009, **48**, 4598-4601.
27 P. C. Hsu and H. T. Chang, *Chem. Commun.*, 2012, **48**, 3984-3986.
28 P. Zhang, W. Li, X. Zhai, C. Liu, L. Dai and W. Liu, *Chem. Commun*., 2012, **48**, 10431-10433.
29 H. Zheng, Q. Wang, Y. Long, H. Zhang, X. Huang and R. Zhu, *Chem. Commun.*, 2011, **47**, 10650-10652.
30 Y. Fang, S. Guo, D. Li, C. Zhu, W. Ren, S. Dong and E. Wang, *ACS Nano*, 2012, **6**, 400-409.
31 B. De and N. Karak, *RSC Adv.*, 2013, **3**, 8286-8290.
32 A. C. Ferrari, *Solid State Commun.*, 2007, **143**, 47-57.
33 Y. Li, Y. Hu, Y. Zhao, G. Shi, L. Deng, Y. Hou and L. Qu, *Adv. Mater.*, 2011, **23**, 776-780.
34 Z. Kang, E. Wang, B. Mao, Z. Su, L. Gao, S. Lian and L. Xu, *J. Am. Chem. Soc.,* 2005, **127**, 6534-6535.
35 L. B. Biedermann, M. L. Bolen, M. A. Capano, D. Zemlyanov and R. G. Reifenberger, *Phys. Rev. B,* 2009, **79**, 125411.
36 Y. Zhong, F. Peng, F. Bao, S. Wang, X. Ji, L. Yang, Y. Su, S. T. Lee and Y. He, *J. Am. Chem. Soc*., 2013, **135**, 8350-8356.
37 Y. Zhong, F. Peng, X. Wei, Y. Zhou, J. Wang, X. Jiang, Y. Su, S. Su, S. T. Lee and Y. He, *Angew. Chem. Int. Ed.*, 2012, **51**, 8485-8489.
38 K. U. Ingold, *Acc. Chem. Res.*, 1969, **2**, 1-9.
39 Z. Luo, Y. Lu, L. A. Somers and A. T. C. Johnson, *J. Am. Chem. Soc.*, 2009, **131**, 898-899.
40 W. Kwon and S. W. Rhee, *Chem. Commun*., 2012, **48**, 5256-5258.
41 S. Zhu, J. Zhang, C. Qiao, S. Tang, Y. Li, W. Yuan, B. Li, L. Tian, F. Liu, R. Hu, H. Gao, H. Wei, H. Zhang, H. Sun and B. Yang, *Chem. Commun.,* 2011, **47**, 6858-6860.
42 Y. He, Y. Zhong, F. Peng, X. Wei, Y. Su, Y. Lu, S. Su, W. Gu, L. Liao and S. T. Lee, *J. Am. Chem. Soc.*, 2011, **133**, 14192-14195.
43 L. Bao, Z. L. Zhang, Z. Q. Tian, L. Zhang, C. Liu, Y. Lin, B. Qi and D. W. Pang, *Adv. Mater.*, 2011, **23**, 5801–5806.
44 R. Jakubiak, C. J. Collison, W. C. Wan, L. J. Rothberg and B. R. Hsieh, *J. Phys. Chem. A,* 1999, **103,** 2394-2398.
45 J. Peng, W. Gao, B. K. Gupta, Z. Liu, R. R. Aburto, L. Ge, L. Song, L. B. Alemany, X. Zhan, G. Gao, S. A. Vithayathil, B. A. Kaipparettu, A. A. Marti, T. Hayashi, J. J. Zhu and P. M. Ajayan,, *Nano Lett.*, 2012, **12**, 844-849.
46 Q. Wang, H. Zheng, Y. Long, L. Zhang, M. Cao and W. Bai, *Carbon*, 2011, **49**, 3134-3140.
47 A. Krueger, *Chem. Eur. J.*, 2008, **14**, 1382-1390.
48 H. C. Chang, in *Nanodiamonds: Applications in Biology and Nanoscale Medicine,* ed. D. Ho, Springer, 2008, ch. 6, 127-150.
49 F. Erogbogbo, K. T. Yong, I. Roy, R. Hu, W. C. Law, W. Zhao, H. Ding, F. Wu, R. Kumar, M. T. Swihart and P. N. Prasad, *ACS Nano,* 2011, **5**, 413-423.
50 F. Erogbogbo, K. T. Yong, I. Roy, G. Xu, P. N. Prasad and M. T. Swihart *ACS Nano*, 2008, **2**, 873-878.
51 Y. He, Y. Zhong, F. Peng, X. Wei, Y. Su, Y. Lu, S. Su, W. Gu, L. Liao and S. T. Lee, *J. Am. Chem. Soc.*, 2011, **133**, 14192-14195.
52 Y. Zhong, F. Peng, F. Bao, S. Wang, X. Ji, L. Yang, Y. Su, S. T. Lee and Y. He, *J. Am. Chem. Soc.*, 2013, **135**, 8350-8356.
53 C. Liu, P. Zhang, F. Tian, W. Li, F. Li and W. Liu, *J. Mater. Chem.*, 2011, **21**, 13163-13167.
54 Z. Mao, Z. Liu, L. Chen, J. Yang, B. Zhao, Y. M. Jung, X. Wang and C. Zhao, *Anal. Chem.,* 2013, **85**, 7316-73.